NIH-PA Author Manuscript
NIH-PA Author Manuscript

NIH Public Access
Author Manuscript
Ultrasound Med Biol. Author manuscript; available in PMC 2009 May 8.

Published in final edited form as:
Ultrasound Med Biol. 2007 September ; 33(9): 1463–1467. doi:10.1016/j.ultrasmedbio.2007.03.011.

Effect of Lesion Boundary Conditions on Axial Strain Elastograms: A Parametric Study

Arun Thitaikumar[1,2] and **Jonathan Ophir**[1]

1 *The University of Texas Medical School, Department of Diagnostic and Interventional Imaging, Ultrasonics Laboratory, Houston, Texas, USA*

2 *University of Houston, Electrical and Computer Engineering Department, Houston, Texas, USA*

Abstract

Ultrasound elastograsphy produces strain images of compliant tissues under quasi-static compression. When a material is compressed, there are several parameters that affect the stress-distribution, and hence the strain distribution in the material. The state of bonding of an inclusion to the background material is a critical parameter. Heretofore in the field of elastography, the inclusion was considered to be firmly bonded to the background material and analytical solutions were derived for the elasticity problem involving simple geometries like circular inclusion (for 2D) and spherical inclusion (3D). Under these conditions, simple analytical expressions relating the strain contrast to the modulus contrast were derived. However, it is known that the state of bonding of some tumors to their surrounding tissues depends on the type of the lesion. For example, benign lesions of the breast are known to be loosely bonded to the surrounding tissue, while malignant breast lesions are firmly bonded. In this study we perform a parametric study using Finite Element Modeling (FEM) to investigate the validity of the analytical expression relating the strain contrast to the modulus contrast, when the state of bonding at the inclusion/background interface spans a large dynamic range. The results suggest that estimated modulus contrast using the analytical expression is sensitive to the region of interest within the inclusion that is considered in the computation of the strain contrast. By considering the inclusion region lying along the axis of lateral symmetry instead of whole region of the inclusion, the estimated modulus contrast (obtained using the analytical expression present in the literature) can be computed to within a systematic error of 10% of the actual modulus contrast. Additional estimation errors are expected to accrue in experimental and *in-vivo* conditions.

Keywords

Bonding; Contrast Transfer Efficiency; Elastography; Modulus Contrast; Strain Contrast; Ultrasound

INTODUCTION

Elastography is a technique that produces images (elastograms) that map the strain experienced by tissue elements subjected to a quasi-static compression (Ophir et al. 1991). Ultrasound elastography typically produces high resolution axial strain elastograms due to high sampling

Contact: Jonathan Ophir, The University of Texas Medical School, Department of Diagnostic and Interventional Imaging, Ultrasonics Laboratory, 6431 Fannin St., Houston, TX 77030, USA, 713.500.7686 Direct, 713.500.7694 Fax, Email: E-mail: Jonathan.Ophir@uth.tmc.edu.

possible in that direction and the ability to use the ultrasound transducer as a tissue compression device. It has been recently shown that modulus contrast approximates the inverse of strain contrast under certain conditions (Srinivasan et al. 2004). This relationship justifies the use of an inverse strain image as a first approximation for a modulus image under certain conditions.

Prior literature reports have investigated the relationship between the strain contrast and the modulus contrast (Ponnekanti et al. 1995; Kallel et al. 1996; Bilgen and Insana 1998). Ponnekanti et al. (1995) described this relationship in terms of contrast transfer efficiency (CTE), defined as the ratio of estimated modulus contrast from elastogram (as inverse of strain contrast) to actual modulus contrast. Later, Kallel et al. (1996) reported an analytic study (2D) on the fundamental limitations on the CTE in elastography. They reported a closed form expression to estimate the modulus contrast from the observed strain contrast viz.

$$\frac{1}{C_s}=\left[\frac{(1-2\nu)}{C_m+(1-2\nu)}+\frac{2}{1+C_m(3-4\nu)}\right] \tag{1}$$

Where, C_s is the strain contrast, C_m is the corresponding Young's modulus contrast, and υ is the Poisson's ratio of both the inclusion and background. For incompressible materials (υ = 0.5), eqn (1) reduces to

$$\frac{1}{C_s}=\frac{2}{1+C_m} \tag{2}$$

Bilgen and Insana (1998) reported a similar study, but for a 3D situation. In all these studies it was assumed that the inclusion was firmly bonded to the background material. However, this assumption may not always hold. In fact, in the case of breast tumors, the literature suggests the existence of differences in the way that benign tumors and malignant tumors are bonded to the surrounding tissues (Chen et al. 1995). Breast fibroadenomas are loosely bonded to their surrounding tissue and possess strong mobility and slip upon palpation (Fry 1954). Breast carcinomas are thought to be firmly bonded to the background due to the formation of stellate boundaries, whereas fibroadenomas are thought to be loosely bonded to the background due to their smooth boundaries (Fry 1959; Chen et al. 1995; Garra et al. 1997; Bamber et al. 1988; Ueno et al. 1988). The nature of the bonding of the lesion to the background has been related to differences in lesion mobility (Bamber et al. 1988; Ueno et al. 1988; Konofagou et al. 2000).

In a recent report (Thitaikumar et al. 2006), we recognized the need to obtain an estimate of the modulus contrast for an inclusion that is loosely bonded to the inclusion. The analytic expression derived in Kallel et al. (1996) and presented in eqn (2) seemed attractive due to its simple form. This expression allows estimating the modulus contrast using the strain contrast measured from axial elastograms. However, as mentioned earlier it was derived under the assumption that the inclusion was firmly bonded to the surrounding. Therefore, the present objective was to study the validity of this expression when the assumption of firm bonding at the inclusion/background interface does not strictly hold. This was investigated using Finite Element Modeling (FEM) based parametric study by changing one model parameter at a time, as explained in the following section.

METHODS

In this study, we have modeled the tissue region as a plane-strain problem with a circular inclusion appearing in the center of a square region of interest. This can be thought of as a cross-section perpendicular to the axis of a cylindrical inclusion at the center of a cube. The assumptions for the material properties and boundary conditions are taken from the literature (Fung 1993) and are 1. the inclusion and background are incompressible elastic materials (Poisson's ratio ~0.495); and 2. slip boundary conditions exist at the bottom of the cube.

The elastographic strain images depend on tissue mechanical properties (such as modulus and Poisson's ratio) and other controlling factors (such as geometry, interfacial bonding conditions, modulus contrast, applied strain and the external boundary conditions). In this work, we compare the estimated modulus contrast (derived from the strain contrast in the axial strain elastogram and from eqn (2)) and the true modulus contrast for a circular inclusion with varying degrees of inclusion/background bonding. The influence of other controlling factors, like the applied axial strain and the inclusion-background modulus contrast on eqn (2) was also studied when the inclusion was loosely bonded.

In order to study the influence of the applied axial strain, a 40 mm × 40 mm phantom with a circular inclusion at the center was generated using the finite element analysis software ANSYS® (Ansys Inc, Canonsburg, PA, USA) running on a windows-based personal computer. The inclusion was twice stiffer than the background and had a diameter of 10 mm. To model a loosely bonded inclusion, we used what is known as *contact elements*. These elements have no physical dimension but have an attribute called the *coefficient of friction*. The coefficient of friction for the contact elements can be varied from 0 (completely de-bonded) to 1. For this study, we used a representative case of a loosely bonded inclusion, modeled with a friction coefficient of 0.01. The phantom was meshed with quadrilateral elements of 8 nodes, 4 nodes at the corners of the quadrilateral and 1 more node at the mid-point of each side. These elements are preferred for plane strain problems (Yound and Budynas 2002, pp-76). The finite element phantom was subjected to axial compression ranging from 0.5% to 5%.

In order to study the influence of modulus contrast, five different software phantoms were constructed. The modulus contrasts between the inclusion and the background were 2, 3, 5, 7 and 10. Here again, we used a representative case of loosely bonded inclusion, modeled with a friction coefficient of 0.01. Each of these phantoms was subjected to an axial compressive strain of 1%. Note that similar studies for the case of firmly bonded inclusion have been reported previously in Ponnekanti et al. (1995) and Kallel et al. (1996).

To study the effect of the degree of bonding, seven phantoms with loosely bonded inclusion were generated, each with a different coefficient of friction. The values for the coefficient of friction ranged from 0.01 to 1. In addition, an eighth phantom with a firmly bonded inclusion was also generated. Note that a firmly bonded inclusion was built in FEM without the use of contact elements. However, one can intuitively think of a firmly bonded inclusion as having infinite coefficient of friction at the inclusion-background interface, if contact elements are used. As shown later in the results section, for a coefficient of friction value of 1 the stress transfer (and hence strains) from background to inclusion tracks that of a firmly bonded inclusion. The inclusions in all of these cases were twice stiffer than the background. Each of the eight phantoms was subjected to an axial compressive strain of 1%.

In order to estimate the modulus contrast using eqn (2), we need to estimate the strain contrast first. The strain contrast can be estimated as the ratio of strain in the background to strain in the target. From the axial elastograms we select two regions of interest (ROI), one from the background and the other from the inclusion. The ROI from the background was selected as a square box of pixels of 8 mm × 8 mm size and 5 mm from the top left corner of the phantom (shown as dashed-white box in figure 1). This region was selected to reduce the effects of strain concentration around the inclusion (Timoshenko and Goodier 1970). It is known that the axial strain distribution inside the inclusion is uniformly distributed only for the case of firmly bonded inclusion (Ru 1998;Sudak et al. 1999). Therefore, we considered two separate ROIs from the inclusion to see which one affected the modulus contrast estimation the least. These ROIs are given below,

1. The whole area of the inclusion (ROI 1)
2. The inclusion region lying along the axis of lateral symmetry (ROI 2)

The mean strain values in the ROIs from the background and the inclusion were used to compute the observed strain contrast (C_s) as $\frac{S_b}{S_i}$, where S_b and S_i are the mean strain values in the ROIs from background and the inclusion, respectively. The modulus contrast was estimated using eqn 2. Figure 1 shows the axial strain image for the case of a firmly bonded and loosely bonded inclusion. It also illustrates the ROI considered for the background (dashed-white box) and the ROI 2 (dashed- white line). The effect of each of the parameters is discussed separately in the results section below.

RESULTS

Applied axial strain

Figure 2 shows a plot of estimated modulus contrast as a function of applied axial strain. As can be seen from the figure, the estimated modulus contrast is dependent on the way we choose the ROI to compute the strain contrast. Clearly, the estimated modulus contrast when ROI 2 is considered (i.e., the inclusion region lying along the axis of lateral symmetry) is closer to the actual modulus contrast value of 2 compared to when ROI 1 is used. The estimated modulus contrast remains essentially constant with applied axial strain. This is not surprising because the strain contrast (and hence the estimated modulus contrast) is determined only by the inherent modulus contrast at any applied strain in the FEM.

Modulus contrast

Figure 3 shows a plot of the estimated modulus contrast as a function of actual modulus contrast when the inclusion was loosely bonded to the background with a coefficient of friction value of 0.01. Here again, notice that the estimated modulus contrast is sensitive to the ROI chosen. As in the case of the applied axial strain, the estimated modulus contrast is close to the actual modulus contrast when using ROI 2.

Coefficient of friction

So far we have considered only a representative case of loosely bonded inclusion. It is of interest to see how different degrees of bonding affect the modulus estimation using eqn 2. Figure 4 shows the plot of estimated modulus contrast as a function of the coefficient of friction. The coefficient of friction studied ranges from a value of 0.01 to firmly bonded case. Observe that the x-axis (axis with the coefficient of friction values) is not continuous. As mentioned earlier, the firmly bonded inclusion can be thought to have an infinite coefficient of friction. It can be seen that as the coefficient of friction increases, the estimated modulus contrast approaches the actual modulus contrast and is slightly overestimated in the case of firmly bonded case. The slight overestimation may be due to FE computation. However, notice that when we choose the ROI appropriately, the estimated modulus contrast is within 10% of the actual modulus contrast (in this example it is in the range of 2 ±0.2). Also, when the inclusion is loosely bonded, the strain distribution inside the inclusion is not uniform (Ru 1998;Sudak et al. 1999) and the stiff inclusion experiences minimal strain at the lateral edges (see figure 1b). Therefore, the strain contrast (and hence the estimated modulus contrast) is overestimated when ROI 1 is considered.

DISCUSSION AND CONCLUSIONS

In the field of elastography, one of the assumptions commonly made is that an inclusion is firmly bonded to the background material. Apart from FEM and experimental studies, analytic expressions have also been derived for the elasticity problem (Ponnekanti et al. 1995; Kallel et al. 1996; Bilgen and Insana 1998; Kallel et al. 2001). The analytical expression relating the observed strain contrast and the modulus contrast was later verified experimentally using gelatin-based phantoms (Kallel et al. 2001). As mentioned earlier, the objective of the present study is to investigate the validity the above mentioned analytic expression (eqn. 2), when the assumption on inclusion/background firm bonding does not hold.

We have found that the choice of ROI within the inclusion plays an important role in determining how close we can estimate the modulus contrast to the actual modulus contrast using eqn (2). We have shown that by considering the ROI to be a portion of the inclusion lying along the axis of lateral symmetry, one can estimate modulus contrast to within 10% of the actual modulus contrast. This was the case over a range of degree of bonding considered, and at a modulus contrast of two (figure 4). However, from figure 3 we observe that the estimated modulus contrast is close to the actual modulus contrast over the range of values modulus contrasts shown (2–10). Therefore, we conclude that the analytic expression shown in eqn (2) can be used to get a first approximation on the modulus contrast from observed strain contrast in axial elastogram even when the inclusion is loosely bonded to the surrounding. It must be noted that the 10% error figure reported in this paper is an irreducible systematic or accuracy error. Additional estimation errors would be expected to accrue in experimental or *in vivo* conditions, which would be reducible by averaging several independent realizations. By comparison, the error in the estimated modulus contrast can be up to 30% of the actual modulus contrast if ROI 1 (the whole lesion) is considered. For the example shown in figure 4, the estimated modulus contrast is 2.7 compared to an actual modulus contrast of 2, when the inclusion is loosely bonded (at a coefficient of friction value of 0.01). It must be realized that a limitation of this technique is that ROI 2 may not have enough pixels to obtain a stable mean value of the strain estimates. However, improvements in Signal-to-Noise Ratio and large inclusion sizes may facilitate the computation of ROI 2 with less difficulty due to a reduction in the variance of the estimates.

Acknowledgements

This work was supported in part by NIH program project grant P01-EB02105–12 awarded to the University of Texas Medical School at Houston. The author was also supported in part by the electrical and computer engineering department, University of Houston through a teaching assistantship. The authors would like to thank the anonymous reviewers for their inputs.

References

Bamber JC, De Gonzalez L, Cosgrove DO, Simmons P, Davey J, McKinna JA. Quantitative evaluation of real-time ultrasound features of the breast. Ultrasoud Med Biol 1988;14 (1):81–87.

Bilgen M, Insana MF. Elastostatics of a spherical inclusion in homogeneous biological media. Phys Med Biol 1998;43:1–20. [PubMed: 9483620]

Chen EJ, Adler RS, Carson PL, Jenkins WK, O'Brien WD Jr. Ultrasound tissue displacement imaging with application to breast cancer. Ultrasound Med Biol 1995;21(9):1153–62. [PubMed: 8849830]

Fry KE. Benign Lesions of the Breast. CA Cancer J Clin 1954;4:160–1.

Fung, YC. Biomechanics-Mechanical properties of living tissues. New York: Springer- Verlag; 1993.

Garra BS, Céspedes I, Ophir J, Spratt RS, Zuurbier RA, Magnant CM, Pennanen MF. Elastography of breast lesions: initial clinical results. Radiology 1997;202:79–86. [PubMed: 8988195]

Kallel F, Bertrand M, Ophir J. Fundamental limitations on the contrast-transfer efficiency in elastography: An analytic study. Ultrasound Med Biol 1996;22 (4):463–70. [PubMed: 8795173]

Kallel F, Prihoda CD, Ophir J. Contrast-transfer efficiency for continuously varying tissue moduli: simulation and phantom validation. Ultrasound Med Biol 2001;27(8):1115–25. [PubMed: 11527598]

Konofagou EE, Harrigan T, Ophir J. Shear strain estimation and lesion mobility assessment in elastography. Ultrasonics 2000;38:400–4. [PubMed: 10829696]

Ophir J, Céspedes I, Ponnekanti H, Yazdi Y, Li X. Elastography: a method for imaging the elasticity of biological tissues. Ultrasonic Imaging 1991;13(2):111–34. [PubMed: 1858217]

Ponnekanti H, Ophir J, Huang Y, Céspedes I. Fundamental mechanical limitations on the visualization of elasticity contrast in elastography. Ultrasound Med Biol 1995;21(4):533–43. [PubMed: 7571146]

Ru CQ. A Circular Inclusion with Circumferentially Inhomogeneous Sliding Interface in Plane Elastostatics. Trans of the ASME 1998;65:30–8.

Srinivasan S, Krouskop T, Ophir J. Comparing elastographic strain images with modulus images obtained using nanoindentation: preliminary results using phantoms and tissue samples. Ultrasound Med Biol 2004;30(3):329–43. [PubMed: 15063515]

Sudak LJ, Ru CQ, Schiavone P, Mioduchowski A. A Circular Inclusion with Inhomogeneously Imperfect Interface in Plane Elasticity. Journal of Elasticity 1999;55:19–41.

Thitaikumar, A.; Ophir, J.; Krouskop, TA.; Garra, BS. Interface bonding strength in axial-shear strain elastography: A preliminary simulation study. Proceedings of the Fifth International Conference on Ultrasonic Measurement and Imaging of Tissue Elasticity; 2006. p. 54

Timoshenko, SP.; Goodier, JN. Theory of Elasticity. New York: McGraw-Hill; 1970. p. p-92

Ueno E, Tohno E, Soeda S, Asaoka Y, Itoh K, Bamber JC, Blaszczyk M, Davey J, McKinna JA. Dynamic tests in real-time breast echography. Ultrasound Med Biol 1988;14(1):53–57. [PubMed: 3055603]

Yound, WC.; Budynas, RG. Roark's Formulas for Stress and Strain. New York: McGraw-Hill; 2002. p. p-76

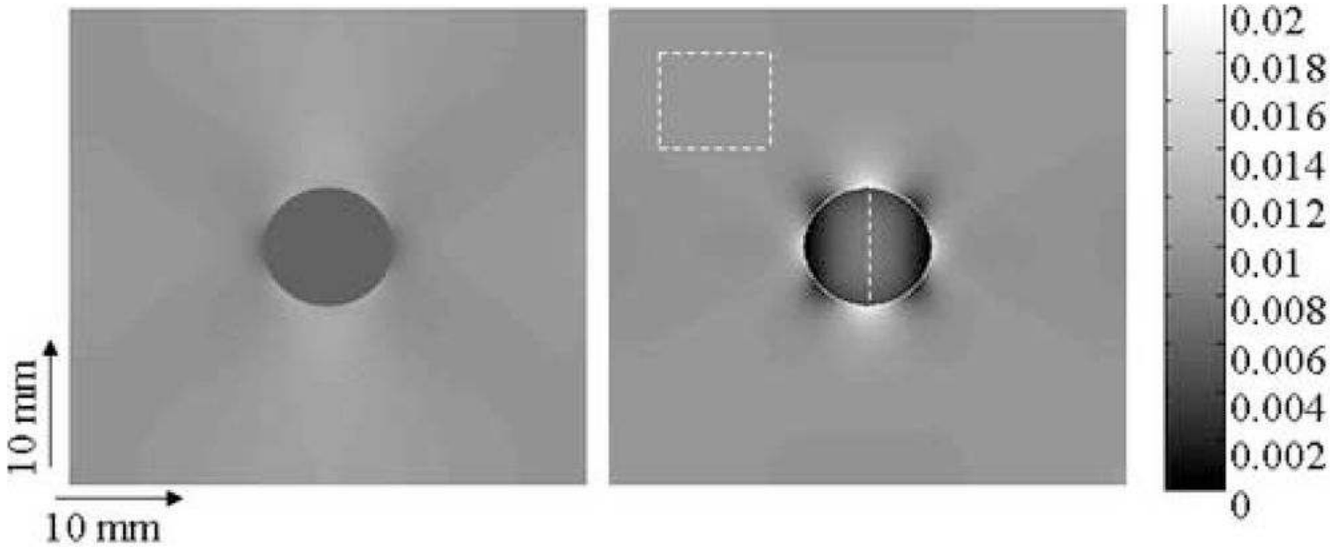

Figure 1.
Axial strain images from FEM of firmly bonded (left) and loosely bonded (right) inclusion. The loosely bonded inclusion was modeled with a friction coefficient of 0.01. The inclusion was twice stiffer than the background and the applied axial strain was 1%. Observe that the axial strain distribution within the inclusion is not uniform in the case of the loosely bonded inclusion. The dashed-white box is the ROI considered from the background and dashed-white line represents the ROI 2.

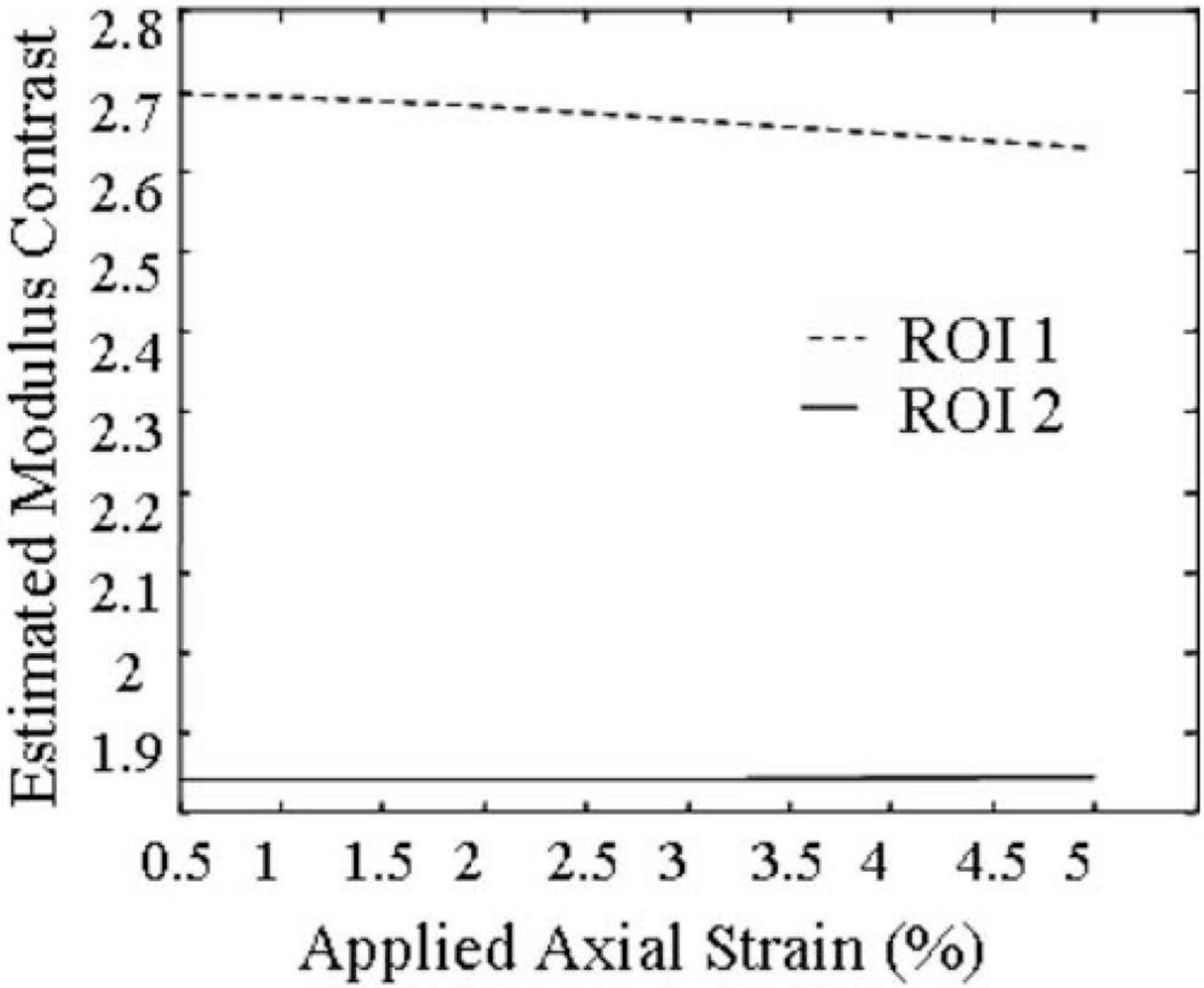

Figure 2.

This plot shows the estimated modulus contrast as a function of the applied axial strain. Observe that the estimated modulus contrast is close to the actual modulus contrast of 2 when ROI 2 is used to compute the strain contrast.

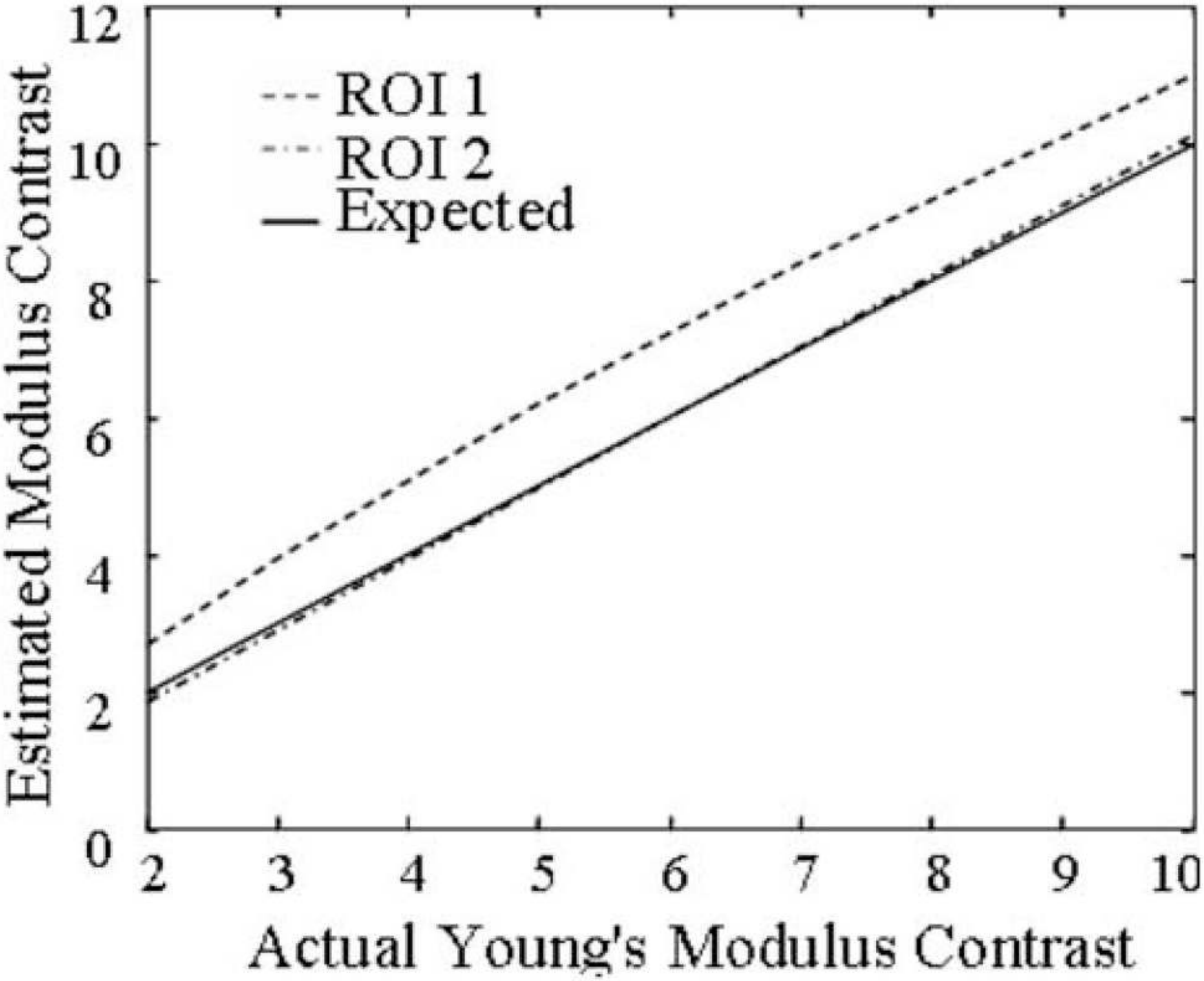

Figure 3.
This plot shows the estimated modulus contrast as a function of the actual modulus contrast. The modulus contrast was estimated from the observed strain contrast using eqn. 2. Observe that the estimated modulus contrast is close to the actual modulus contrast when ROI 2 is used to compute the strain contrast. The inclusion was loosely bonded to the background with a coefficient of friction value corresponding to 0.01.

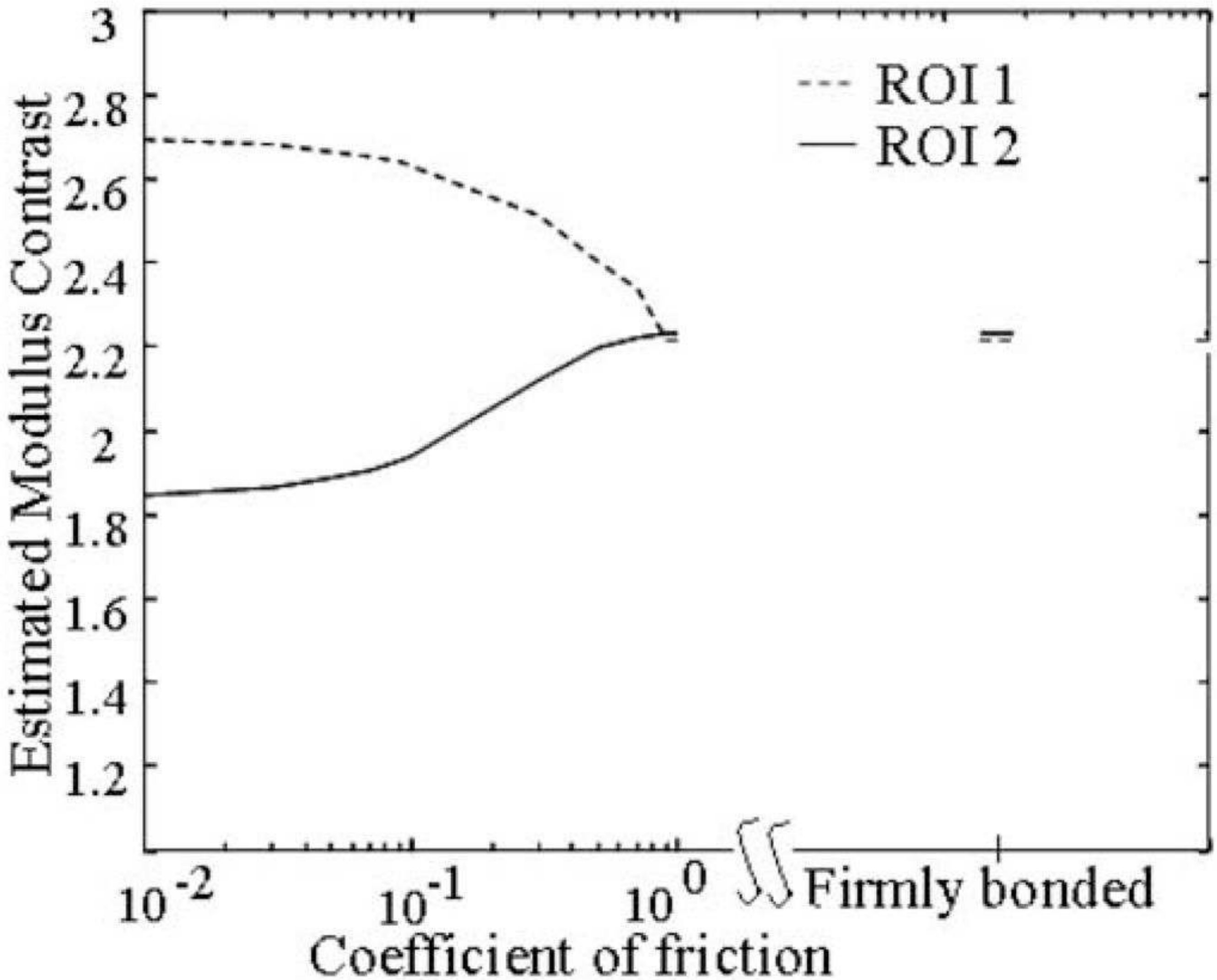

Figure 4.
This plot shows the estimated modulus contrast at various degrees of bonding, modeled using coefficient of friction. The estimated modulus contrast is within +/− 10 % of the actual modulus contrast of 2 when ROI 2 is used to compute the strain contrast.